

## End-to-end distance distributions and asymptotic behaviour of self-avoiding walks in two and three dimensions

This article has been downloaded from IOPscience. Please scroll down to see the full text article.

1995 J. Phys. A: Math. Gen. 28 1271

(<http://iopscience.iop.org/0305-4470/28/5/015>)

View [the table of contents for this issue](#), or go to the [journal homepage](#) for more

Download details:

IP Address: 171.66.16.68

The article was downloaded on 02/06/2010 at 02:16

Please note that [terms and conditions apply](#).

# End-to-end distance distributions and asymptotic behaviour of self-avoiding walks in two and three dimensions

R Everaers†§, I S Graham†† and M J Zuckermann†

† Department of Physics, McGill University, Rutherford Building, 3600 University Street, Montréal, Québec, Canada H3A 2T8

‡ National Research Council, Industrial Materials Institute, 75 De Mortagne Boulevard, Boucherville, Québec, Canada J4B 6Y4

Received 14 June 1994

**Abstract.** We use Monte Carlo methods to study the reduced moments and full end-to-end distance distributions of self-avoiding walks in two and three dimensions. We find that the reduced moments scale with length via  $\delta_{pq} = A + B/N^{\Delta_{pq}}$  with corrections to the scaling exponents that vary with the order of the moment. We also find that the complete end-to-end distance distributions are well described by a Redner–des Cloizeaux (RdC) model  $q_N(x) = C x^{\theta_N} \exp(-(Kx)^{t_N})$  [1, 2],  $x$  being the rescaled length. We develop a method that allows reliable estimation of the exponents  $\theta_N$  and  $t_N$  from the extrapolated reduced moments and use this method to extrapolate to chain lengths beyond those investigated here. We find that, in three dimensions, the optimal  $t_N$  for  $N > 1000$  is smaller than the theoretically expected value  $t = 2.445$ . This implies that care must be taken in using the RdC ansatz to interpret the behaviour of self-avoiding walks, even in the asymptotic limit.

## 1. Introduction

Self-avoiding walks, or SAWs, are well known in the literature [3] as models for polymer chains in a good solvent. This is because they are the simplest model that retains the essential physics of the problem: that a polymer is a flexible chain which cannot self-intersect. Because of the latter property analytic treatments are exceedingly difficult: we summarize the known results below. Due to these problems computer simulations play an important role in the field [4].

In this paper we study the full end-to-end distance distribution of SAWs in two and three dimensions, for several chain lengths  $N$ . We are interested in answering two questions: is this distribution well modelled by an ansatz due to Redner and des Cloizeaux [1, 2], and how do the properties scale in the large- $N$  limit? To provide a framework for this, we first present a review of the relevant theory of the scaling properties of polymers.

The measurable quantities of SAWs are known to obey some simple scaling laws [3]. As a function of chain length  $N$  the root-mean-square (RMS) end-to-end distance,  $R_N$ , and

§ Present address: Institut für Festkörperforschung, Forschungszentrum Jülich, Postfach 1913, D-52425 Jülich, Germany.

|| E-mail address: ever@ifff042.iff.kfa-juelich.de

**Table 1.** Theoretical and numerical estimates of the exponents  $\nu$ ,  $t$  and  $\theta$ , in the large- $N$  limit. The literature values for  $t$  and  $\theta$  were calculated via (5), (4) and (11), respectively, using the given values of  $\nu$  and  $\gamma$ . The results in 2D are considered exact.

	$\nu$	$\gamma$	$t$	$\theta$	$g$
2D	0.75 [22]	$\frac{43}{32}$ [22]	4	$\frac{11}{24}$	$\frac{5}{8}$
3D	0.592(1)[23, 24, 16]	1.162(2) [25]	2.451(6)	0.274(4)	0.279(7)

the number of  $N$ -step SAWs,  $c_N$ , (equivalent, in the absence of interactions, to the chain partition function  $\mathcal{Z}_N$ ) obey

$$R_N = \sqrt{\langle r^2 \rangle} \sim N^\nu \quad (1)$$

$$(\mathcal{Z}_N =) c_N \sim \mu^N N^{\gamma-1} \quad (2)$$

in the limit of large  $N$ . The exponents  $\gamma$  and  $\nu$  are believed to be universal for a given dimension, while  $\mu$ , the connective constant, is characteristic of the lattice. Accepted numerical values are summarized in table 1.

We focus on the chain end-to-end distance distribution  $p_N(\mathbf{r})$ , where  $\mathbf{r}$  joins the two ends of the chain.  $p_N(\mathbf{r})$  is expected to have the scaling form [3]

$$p_N(\mathbf{r}) = \frac{1}{R_N^d} q(\mathbf{x}) \quad (3)$$

with  $\mathbf{x} = \mathbf{r}/R_N$ . This implies that the RMS end-to-end distance is the only relevant length scale. For free chains there are some elegant scaling arguments [3, 5], confirmed by more rigorous approaches [2, 6–8] for limiting cases of the asymptotic distribution  $q(\mathbf{x})$ . Power-law behaviour  $q(\mathbf{x}) \sim x^\theta$  is predicted in the limit  $x \rightarrow 0$  (endpoints close together), with  $\theta$  given by

$$\theta = \frac{\gamma - 1}{\nu} \quad (4)$$

When the endpoints are far apart, namely  $x \gg 1$ , the distribution is expected to decay via  $q(\mathbf{x}) \sim x^g \exp(-[Kx]^t)$ , with exponents  $t$  and  $g$  given by

$$t = \frac{1}{1 - \nu} \quad (5)$$

$$g = \frac{1 - \gamma + \nu d - d/2}{1 - \nu} \quad (6)$$

Recently Stepanow [28] suggested the existence of two additional length scales  $r^*$  and  $r^{**}$ , below and above which the scaling suggested by (4)–(6) should be violated. In particular, he predicts a different dependence,  $q(\mathbf{x}) \sim \exp(-x)$ , for large distances between the endpoints. This conjecture has yet to be verified.

The exponential term along with the exponent defined in (5) is often called the Fisher–Pincus law. Current best estimates for the exponents  $\gamma$  and  $\nu$  (the 2D results are exact), and the corresponding values of  $\theta$ ,  $g$  and  $t$  are summarized in table 1. It turns out that the exponents  $\theta$  and  $g$  are nearly the same. In 3D the two agree to within the estimated errors, while in 2D the difference is  $\frac{1}{6}$ , which is still quite small. This led Redner [1] and des Cloizeaux [2] to conjecture that the function

$$q(\mathbf{x}) = C x^\theta e^{-(Kx)^t} \quad (7)$$

should be a good approximation of the entire scaled end-to-end distance distribution, with  $t$  and  $\theta$  given by (5) and (4). In this Redner–des Cloizeaux (RdC) ansatz,  $K$  and  $C$  are not

additional parameters but are fixed by two conditions: (i) that the distribution is normalized ( $\int x^{d-1} q(|x|) dx \equiv 1$ ) and (ii) that the second moment was chosen as the scaling length (equation (1)), namely ( $\int x^{d+1} q(|x|) dx \equiv 1$ ). These conditions yield

$$K^2 = \frac{\Gamma([\theta + d + 2]/t)}{\Gamma([\theta + d]/t)} \quad (8)$$

$$C = t \frac{\Gamma^{(\theta+d)/2}([\theta + d + 2]/t)}{\Gamma^{(\theta+d+2)/2}([\theta + d]/t)}. \quad (9)$$

Previous simulation work largely supported this conjecture (see [9] for a summary of earlier results). However, until recently only the reduced moments

$$\delta_{pq} = \langle r^p \rangle / \langle r^q \rangle^{p/q} \quad (10)$$

could be measured to reasonable precision. These data appeared to indicate that  $\delta_{pq} \sim 1/N$ . Extrapolations based on this assumption yielded estimates for the reduced moments in good agreement with those predicted by the RdC distribution using the theoretically expected exponents. These moments are calculated from the RdC ansatz via the formula [9, equation (23)]

$$\delta_{pq} = \Gamma([\theta + d + p]/t) \Gamma([\theta + d]/t)^{p/q-1} \Gamma([\theta + d + q]/t)^{-p/q}. \quad (11)$$

Recently two groups directly measured the distribution function, in three dimensions, and reported good agreement with the RdC ansatz [10, 11]. In particular, Eizenberg and Klafter [11] investigated chains of up to several thousand segments in length. From a comparison of the binned distributions they concluded that, to the precision of their results, the asymptotic shape had been reached. However, they fit the data to the RdC ansatz (7) assuming that the exponent  $t$  is given by (5), namely  $t = 2.445$ . As a result they did not report any model-independent quantities such as the reduced moments.

The remainder of the paper is organized as follows. The next section contains a discussion of our Monte Carlo simulation methods. This is followed by our simulation results, where we determine both the reduced moments and the complete end-to-end distributions for free 2D and 3D chains of several lengths  $N$ . We find that the reduced moments scale with chain length via  $A_{pq} + B_{pq}/N^{\Delta_{pq}}$ , with exponents that vary with the order of the moment. In particular, we find  $\Delta_{pq} < 1$  and thus a slower approach to the asymptotic shape than previously expected. We also find that the full end-to-end distributions are well modelled by the RdC ansatz (7) if we use chain-length-dependent exponents  $t_N$  and  $\theta_N$ . To examine the behaviour of these exponents in the large- $N$  limit we develop a method that takes advantage of our reliable extrapolations of the reduced moments  $\delta_{pq}$ . This method accurately reproduces our direct fits to the full distributions, and is shown to be consistent with the measurements of other researchers. Most importantly we find that, in 3D, the extrapolated exponents  $t = 2.39 \pm 0.03$ , noticeably different from the theoretically expected value 2.445. We conclude with a discussion of the implications of these results.

## 2. Methods

Simulation work on SAWs has followed two distinct approaches. The first method is to start from an initial site on a lattice and walk randomly to generate a fixed length walk. If the walk does not contain any forbidden self-intersections, it can be analysed, and the process repeated. The advantage is that the measurements are uncorrelated. The disadvantage is that the probability of randomly generated walks being self-avoiding decreases exponentially

with chain length (attrition). More efficient are dimerization methods [12–14], which we use to obtain equilibrated initial configurations. The idea is to generate two SAWs of half the desired length and then to concatenate them. If this fails to yield a SAW both halves are discarded and another attempt is made. This algorithm is applied recursively down to a length where attrition is not a problem.

The most common approach to the simulation of SAWs, and the one we primarily use, is to start with an initial configuration satisfying the boundary conditions and to make small changes to this configuration, following a set of well defined rules. The rules must be chosen so that the sequence is ergodic and that detailed balance is fulfilled. We use the pivot algorithm originally invented by Lal [15] to study SAWs on a cubic lattice. In this algorithm a MC step consists of choosing a point randomly along the chain and applying a symmetry operation of the lattice (reflection or rotation) to the rest of the chain. The result is accepted if no self-intersections occur. As pointed out by Madras and Sokal [16] this leads to relatively short correlation times for global properties of the chain, such as the end-to-end distance. However, it is important to note that this is not the case for local quantities. We worked closely along the lines of [16], and similarly used dimerization to obtain fully equilibrated initial configurations.

To check our programs we simulated short chains using both the pivot and the dimerization algorithm. From exact enumeration exact values for the mean square end-to-end distance are known [17, 18], which were well reproduced by our simulations:

	Exact	Dimerization	Pivot
$N = 20(2D)$	72.077	72.141(73)	72.139(64)
$N = 10(3D)$	16.817	16.799(14)	16.807(14)

We measured the end-to-end distance, the radius of gyration and the components of the latter parallel and perpendicular to the end-to-end vector. To ensure uncorrelated data we first did shorter runs to determine the relaxation times for the quantities under investigation. For free chains they were found to be smaller than seven MC steps for  $N = 10$  and smaller than 30 MC steps for  $N = 240$ . In general, relaxation times were slightly longer in the 2D case. The distance between successive measurements was between three and five times the longest relaxation time, so that our data can be regarded as uncorrelated. In all cases the total number of data points obtained in the production runs with the pivot algorithm was  $5 \times 10^5$  for chains of length  $N = 10, 20, 40, 60, 80, 100, 120, 160, 200$  and 240. To obtain better statistics in the histograms for the end-to-end distance distribution the binning was additionally done at five intermediate time steps.

For comparison we also used the dimerization algorithm to generate data for  $N = 80$  in two dimensions and for  $N = 60$  and 120 in three dimensions. In these cases  $10^5$  data points were obtained, which are uncorrelated due to the nature of the algorithm.

### 3. Results

We first present results for the reduced moments of the end-to-end distance distribution. These data can be directly compared to earlier work and are precise enough to allow for careful extrapolations to the  $N \rightarrow \infty$  limit. We next consider the full distributions  $q(x)$  and examine how well they are described by the R&C ansatz. Lastly we develop a method to test and estimate the best-fit parameters of a model distribution from knowledge of the reduced moments. The advantage here is that the straightforward extrapolations of the reduced moments allow us to obtain reliable estimates for chains in the  $N \rightarrow \infty$  limit.

## 3.1. Reduced moments

Measurements of the mean-square end-to-end distance  $\langle r^2 \rangle$  and the reduced moments  $\delta_{pq}$  are summarized in tables 2 and 3. These compare well to earlier results (see [16–19] for  $\langle r^2 \rangle$  results and [9] for a summary of results on moments) while being significantly more precise. We note also that, where we have both pivot and dimerization data, our results agree to within the statistical error. This consistency is a useful check of our algorithms.

Djordjevic *et al* [20] predicted the following chain-length-dependence of the mean-square end-to-end distance:

$$\langle R^2(N) \rangle = AN^{2\nu} (1 + BN^{-\Delta} + CN^{-1} + \dots). \quad (12)$$

As the  $1/N$  term was found to be small in previous studies [20, 21], only the  $N^{-\Delta}$  term was retained in obtaining the following estimates for  $\nu$ :  $\nu_{2D} = 0.7507 \pm 0.0006$  and  $\nu_{3D} = 0.592 \pm 0.002$ . In 2D the value  $\nu_{2D} = 0.75$  is believed exact [22]. In 3D the best analytical results are  $\nu_{3D} = 0.588$  [23] and  $0.592$  [24], while the best series-extrapolation estimate is  $0.592 \pm 0.002$  [25]. The best estimates from simulation are  $0.592 \pm 0.001$  [16] and  $0.5909 \pm 0.0003$  [11], obtained with walks of several thousand steps [16]. Our results (summarized in table 5) are in excellent agreement with these values. We estimated the leading correction-to-scaling exponent by setting  $\nu$  to the literature values quoted above,

**Table 2.** Root-mean-square end-to-end distance and reduced moments for two-dimensional SAWs. The (d) indicates data generated by the dimerization algorithm. The (R) indicates reduced moments calculated from the fitted Redner–des Cloizeaux distributions (equation (15)) using the exponents given in table 4 (for the relevant chain length). The row labelled  $\Delta$  gives the correction-to-scaling exponent for the growth of  $\langle r^2 \rangle$  (see equation (13)). Reduced moments were extrapolated to  $N \rightarrow \infty$  via  $A + B/N^{\Delta_{pq}}$ ; the exponents  $\Delta_{pq}$  and the extrapolated moments are given in the next two rows. The final two rows give the reduced moment predicted by the RdC ansatz (equation (17)): RdC (1) using the theoretically expected exponents  $t$  and  $\theta$  taken from table 1, while RdC (2) uses our estimates of the exponents obtained by extrapolation of the ratios of reduced moments. These exponents are summarized in table 5.

$N$	$\langle r^2 \rangle$	$\delta(2, 1)$	$\delta(4, 2)$	$\delta(6, 3)$	$\delta(6, 2)$	$\delta(8, 4)$	$\delta(8, 2)$
10	26.282(22)	1.110 35(23)	1.350 20(68)	1.6821(14)	2.1550(27)	2.1114(28)	3.8492(86)
20	72.139(64)	1.124 15(26)	1.394 54(78)	1.7803(17)	2.3427(33)	2.2962(34)	4.466(11)
40	200.09(18)	1.131 09(27)	1.420 02(84)	1.8422(19)	2.4596(37)	2.4219(40)	4.884(13)
60	364.59(34)	1.132 98(28)	1.427 51(86)	1.8621(20)	2.4966(38)	2.4659(42)	5.025(14)
60(R)		1.134 20(22)	1.431 56(74)	1.8716(16)	2.5152(33)	2.4863(31)	5.095(11)
80	559.11(52)	1.134 57(28)	1.433 09(87)	1.8752(20)	2.5221(39)	2.4920(44)	5.118(14)
80(d)	559.8(12)	1.135 20(62)	1.435 9(20)	1.8812(45)	2.5342(88)	2.5013(95)	5.157(32)
100	780.07(73)	1.134 83(28)	1.434 47(88)	1.8796(21)	2.5260(40)	2.5037(45)	5.152(15)
120	1023.14(95)	1.135 51(28)	1.438 24(88)	1.8891(21)	2.5478(40)	2.5220(46)	5.217(15)
120(R)		1.135 38(23)	1.437 69(77)	1.8886(17)	2.5463(35)	2.5234(33)	5.216(12)
160	1571.6(15)	1.135 84(28)	1.439 87(89)	1.8943(21)	2.5569(41)	2.5350(48)	5.256(15)
200	2196.6(21)	1.136 00(28)	1.440 04(89)	1.8953(21)	2.5586(41)	2.5392(48)	5.266(16)
240	2885.6(31)	1.136 30(32)	1.441 6(10)	1.8987(25)	2.5650(47)	2.5470(55)	5.291(18)
240(R)		1.136 30(23)	1.441 30(78)	1.8974(18)	2.5633(35)	2.5413(34)	5.279(13)
$\Delta$	0.79(1)						
$\Delta_{pq}$		1.041 (35)	0.897 (29)	0.794(22)	0.806(24)	0.706(24)	0.716(23)
Extrap.		1.137 36(24)	1.447 5(10)	1.9195(25)	2.6031(49)	2.6031(70)	5.474(22)
	2.5735(44)	5.381 (14)					
RdC (1)		1.140 607	1.458 32	1.9393	2.6448	2.6271	5.587
RdC (2)		1.137 44(28)	1.448 72(60)	1.9196(38)	2.6031(55)	2.592(11)	5.440(27)

**Table 3.** Root-mean-square end-to-end distance and reduced moments for three-dimensional SAWs. The (d) indicates data generated by the dimerization algorithm. The (R) indicates reduced moments calculated from the fitted Redner–des Cloizeaux distributions (equation (15)) using the exponents given in table 4 (for the relevant chain length). The row labelled  $\Delta$  gives the correction-to-scaling exponent for the growth of  $\langle r^2 \rangle$  (see equation (13)). Reduced moments were extrapolated to  $N \rightarrow \infty$  via  $A+B/N^{\Delta_{pq}}$ : the exponents  $\Delta_{pq}$  and the extrapolated moments are given in the next two rows. The final two rows give the reduced moment predicted by the RdC ansatz (equation (17)): RdC (1) using the theoretically expected exponents  $\iota$  and  $\theta$  taken from table 1, while RdC (2) uses our estimates of the exponents obtained by extrapolation of the ratios of reduced moments. These exponents are summarized in table 5.

$N$	$\langle r^2 \rangle$	$\delta(2, 1)$	$\delta(4, 2)$	$\delta(6, 3)$	$\delta(6, 2)$	$\delta(8, 4)$	$\delta(8, 2)$
10	16.807(14)	1.105 83(21)	1.367 88(73)	1.7732(19)	2.2841(33)	2.3527(45)	4.402(12)
20(d)	38.766(42)	1.119 52(28)	1.421 0(10)	1.9079(28)	2.5334(51)	2.6389(71)	5.328(21)
20	38.714(36)	1.119 48(23)	1.420 62(87)	1.9053(25)	2.5296(42)	2.6277(57)	5.303(17)
40	88.841(85)	1.127 53(25)	1.453 60(98)	1.9950(29)	2.6972(52)	2.8364(78)	5.993(23)
60(d)	144.49(31)	1.130 60(58)	1.468 2(23)	2.0378(68)	2.776(12)	2.936(18)	6.328(56)
60	144.29(14)	1.130 50(26)	1.465 9(10)	2.0268(30)	2.7586(55)	2.9048(83)	6.242(25)
60(R)		1.131 04(31)	1.467 6(12)	2.0346(29)	2.7716(58)	2.9321(61)	6.316(23)
80	203.04(20)	1.132 52(26)	1.474 8(10)	2.0513(31)	2.8052(57)	2.9602(85)	6.438(26)
100	265.27(26)	1.133 52(26)	1.478 8(11)	2.0626(32)	2.8268(58)	2.9874(88)	6.533(27)
120(d)	329.89(72)	1.134 48(60)	1.482 2(24)	2.0704(72)	2.843(13)	3.004(20)	6.600(62)
120	329.34(32)	1.134 32(27)	1.482 2(11)	2.0717(32)	2.8445(59)	3.0077(90)	6.608(28)
120(R)		1.134 22(33)	1.482 2(13)	2.0753(31)	2.8490(63)	3.0263(67)	6.649(26)
160	463.71(46)	1.135 51(27)	1.488 2(11)	2.0918(35)	2.8807(63)	3.066(10)	6.790(31)
200	605.24(60)	1.136 26(27)	1.490 7(11)	2.0960(34)	2.8907(62)	3.0684(98)	6.818(30)
240	750.27(75)	1.136 65(27)	1.494 0(11)	2.1084(35)	2.9122(64)	3.103(10)	6.925(31)
240(R)		1.136 75(34)	1.493 6(13)	2.1065(33)	2.9091(66)	3.0982(71)	6.911(28)
$\Delta$	0.50(5)						
$\Delta_{pq}$		0.721 (16)	0.654 (22)	0.592(20)	0.581(20)	0.522(24)	0.487(21)
Extrap.		1.140 10(30)	1.511 0(20)	2.1645(61)	3.024(11)	3.268(21)	7.582(75)
2.974(12)	3.186(19)	7.177 (44)					
RdC (1)		1.138 50(44)	1.502 8(17)	2.1345(45)	2.9617(90)	3.167(10)	7.153(39)
RdC (2)		1.140 42(90)	1.513 45(74)	2.1674(33)	3.0233(21)	3.249(16)	7.442(29)

and fitting for  $\Delta$ . We obtained the fits

$$\sqrt{\langle r^2 \rangle_{2D}} = N^{0.75} (0.7701(9) + 0.37(2)N^{-0.79(3)}) \quad (13)$$

$$\sqrt{\langle r^2 \rangle_{3D}} = N^{0.592(1)} (1.15(2) - 0.175(7)N^{-0.54(10)}) \quad (14)$$

which gave excellent descriptions of the data.

For the reduced moments we made an ansatz similar to (12), namely

$$\delta_{pq}(N) = a_{pq} + b_{pq} N^{-\Delta_{pq}} \quad (15)$$

and tried two different methods: (i) simple  $1/N$  extrapolation (i.e.  $\Delta_{pq} \equiv 1$ ) as used previously [9] and (ii) a variable correction to scaling exponent  $\Delta_{pq}$ . Figure 1 shows our results for the reduced moment  $\delta_{82}$  in three dimensions, including also the results of Bishop and Clarke [9], and values calculated from the fits of Eizenberg and Klafter [11]. While the  $1/N$  extrapolation was compatible with the older data of Bishop and Clarke [9], this function is clearly ruled out by our more precise measurements: the  $1/N$  fit simply does not follow the trend in the data. On the other hand, a model where we allowed the exponents  $\Delta_{pq}$  to depend on  $pq$  gave excellent descriptions of our data. In tables 2 and 3 we have summarized both the best-fit exponents  $\Delta_{pq}$  and the corresponding extrapolated moments.

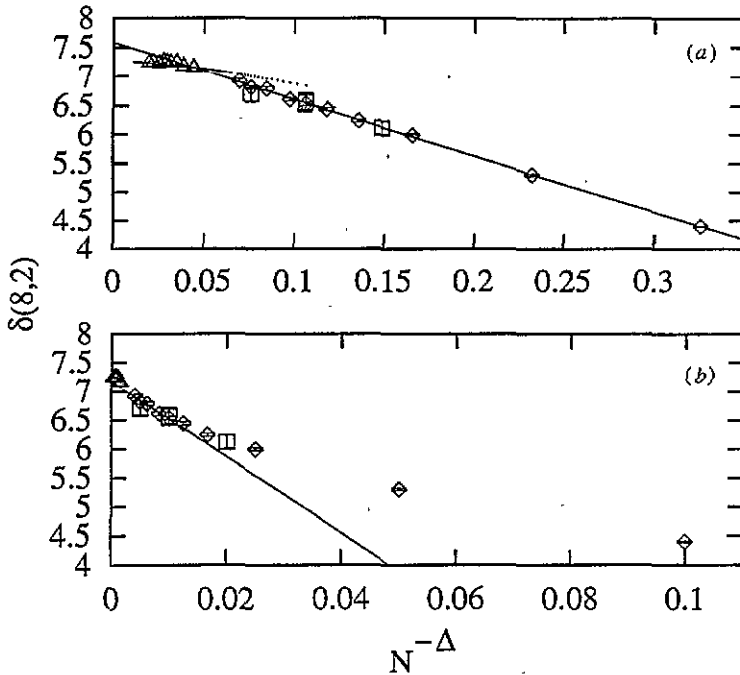


**Figure 1.** Measured reduced moments  $\delta_{82}$ , for  $d = 3$ , as a function of chain length  $N$ . In (a) the data are plotted versus  $N^{-0.487}$ , in (b) versus  $N^{-1}$ . In both cases the best fit to our data is shown as a full line. The figures show data from three sources: our data from table 3 ( $\diamond$ ), the earlier results of Bishop and Clarke [9] ( $\square$ ), and the reduced moments calculated from recent fits of Eizenberg and Klafter [11] (EK) ( $\triangle$ ). The dotted curve shows our estimate for  $\delta_{82}$  calculated from fits to a RdC model with  $\tau = 2.445$ .

We note that there is a pattern in the correction exponents: they are largely independent of  $q$ , with values dropping in roughly equidistant steps with  $p$ .

The ansatz (15) with correction to scaling exponents  $\Delta_{pq}$  is empirical, but was required by the fact that there was no single exponent that reasonably described all the moments. Our results can certainly be trusted as an excellent *interpolation* between our data points, however, the *extrapolation* to large  $N$  is, in principle, open to systematic error. To check this point further we attempted to compare our results to other studies involving longer chains.

In a recent publication Eizenberg and Klafter (EK) [11] determined the end-to-end distance distributions of 3D walks on a cubic lattice in the range  $N = 608$  to  $N = 7200$ . The distributions were fit to a RdC model, with  $\tau$  fixed at the theoretically expected value at large  $N$  (2.445) and with  $K$  and  $\theta$  as fit parameters. Unfortunately, they did not determine the reduced moments, so that we calculated the values included in figure 1 using the RdC expression (11) and their fit results [11, table V].

We find that their data do not support either scaling ansatz. Although the first three data points (smallest  $N$ ) appear in reasonable agreement with our extrapolation, for longer chains the moments bend over to a constant value, indicating that an asymptotic regime is reached at around  $N = 2000$ . We believe that this plateau is unphysical, and that it arises from the assumption  $\tau = 2.445$ , which is apparently incorrect even for these extremely long chains. We discuss this point more fully later in this section.



As a direct check of the RdC model we examined how well it reproduced our extrapolations for the reduced moments. Using the literature values for exponents listed in table 1 and (11) we obtained the reduced moments labelled RdC (1) in tables 2 and 3. There is reasonable qualitative agreement with the extrapolated values, with worst-case deviations of the order of 2%(5%) in 2D(3D). However, given the precision of our extrapolations these predictions are well outside the error estimates, suggesting that the RdC expression, using the accepted exponents, is only approximate, even in the  $N \rightarrow \infty$  limit.

### 3.2. End-to-end distance distributions

In addition to measuring the moments we also measured  $q(x)$  directly, by binning the chain end-to-end distances into a histogram. The raw distributions are quite scattered due to fluctuations in the number of accessible lattice points around the physical volume of the bins. Properly smoothed curves are obtained by correcting for this [10,26,27] instead of using the raw bin volume. There is, however, some arbitrariness in the choice of the histogram widths and positions, along with associated systematic errors. We systematically varied the width and position of the bins under the condition that there were no empty bins. As a result we found that, even for bins of the width of the lattice constant, only the first one or two points of the resulting distributions were sensitive to this choice. For the first bin, however, the effect was so drastic that we excluded this point from subsequent analysis. In our opinion, for the lattice correction to give reliable results, the bins must contain more than just one or two points on the lattice. Our final choice were bins of width 1.5 starting

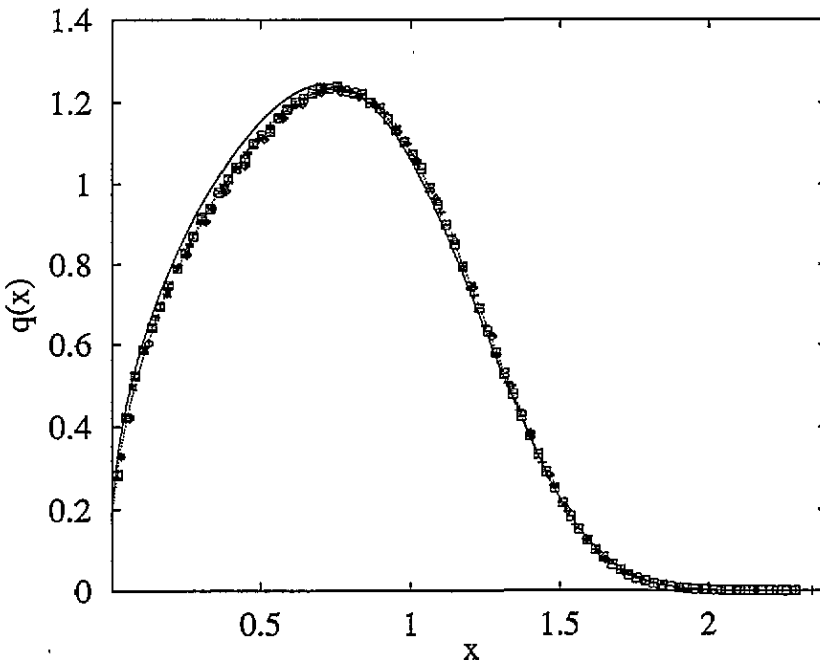


Figure 2. Scaled end-to-end distributions for 2D SAWs. We show data for chain length  $N = 80$  ( $\diamond$ ),  $N = 160$  (+) and  $N = 240$  ( $\square$ ). The full curve represents the RdC distribution with the theoretically predicted exponents from table 1. The dotted curve is the result of fitting these exponents to best match the  $N = 160$  data.

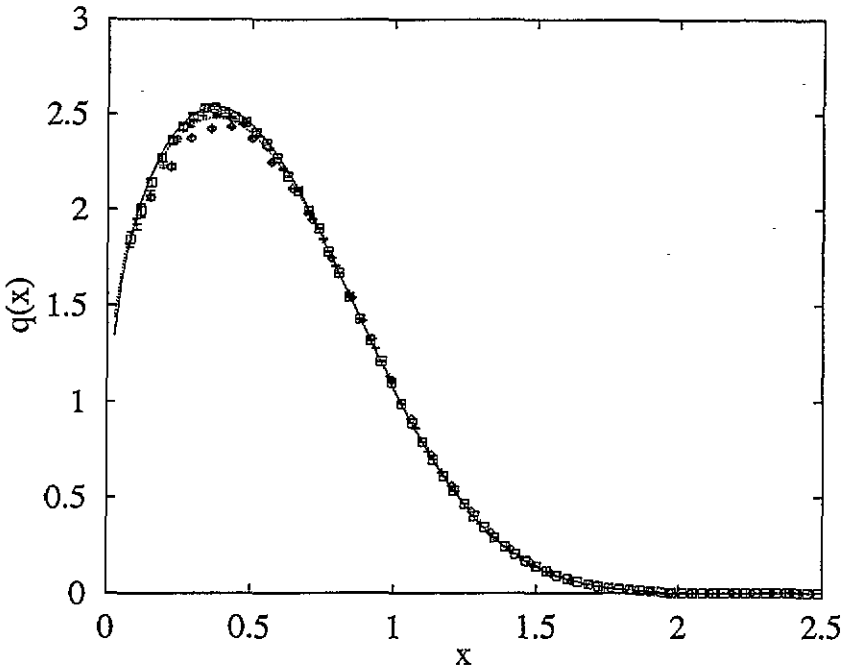


Figure 3. Scaled end-to-end distribution for 3D SAWs. We show data for chain length  $N = 80$  ( $\diamond$ ),  $N = 160$  ( $+$ ) and  $N = 240$  ( $\square$ ). The full curve represents the RdC distribution with the theoretically predicted exponents from table 1. The dotted curve is the result of fitting these exponents to best match the  $N = 160$  data.

at 2.375 in 2D and bins of width 1.0 starting at 1.625 in 3D.

Alternatively Dayantis and Palierne [10] performed the binning *after* dividing the distances by  $N^\nu$ , so that the number of bins is independent of the chain length  $N$ . For  $N = 200$  the first bins covered distances of [0.68, 1.14], [1.14, 1.59], ... on the lattice, while for  $N = 600$  [1.3, 2.17], [2.17, 3.04], ... was used. This has the possible disadvantage that systematic errors for the closest bins may be obscured, as they are different for each chain length studied. In addition the authors made a significant investment of computer time to also obtain good statistics for the closest bins. In a log-log plot they observed that for  $r/N^\nu < 0.1$  their points seemed to follow a different power law. However, they did not take into account the systematic errors due to the discrete lattice which, in this region, can be much larger than the statistical ones. Depending on our choice of the histogram we observed similar effects.

Figures 2 and 3 show superpositions of our scaled end-to-end vector distributions (averaged over angles) and demonstrate the validity of the scaling form (3). Around the *maxima of the distributions we see small, but systematic, variations with the chain length.* This is expected from finite-size considerations. The full curves in these figures show the conjecture of Redner and des Cloizeaux (7), using standard exponents (table 1). The overall appropriateness of the function is remarkable, although there are systematic differences largely due to the finite sizes of the chains.

Our next step was to model the scaled distributions  $q_{2D}(x)$  and  $q_{3D}(x)$  using the Redner-des Cloizeaux ansatz (7), but with  $t_N$  and  $\theta_N$  as adjustable parameters. The purpose was two-fold: first to test the ability of the RdC-expression to describe data for finite-sized

**Table 4.** Effective exponents  $\theta_N$  and  $t_N$  obtained by fitting the complete end-to-end distance distribution to Redner–des Cloizeaux functions (equation (8)). The final row give the result of a simple  $1/N$  extrapolation to  $N \rightarrow \infty$ .

$N$	2D		3D	
	$\theta_N$	$t_N$	$\theta_N$	$t_N$
40	0.473(6)	4.50(2)	0.17(1)	2.83(1)
60	0.461(6)	4.39(2)	0.22(1)	2.71(1)
80	0.459(6)	4.36(2)	0.22(1)	2.66(1)
100	0.472(6)	4.30(2)	0.24(1)	2.62(1)
120	0.474(6)	4.25(2)	0.24(1)	2.60(1)
160	0.469(6)	4.24(2)	0.24(1)	2.57(1)
200	0.474(6)	4.20(2)	0.24(1)	2.54(1)
240	0.471(6)	4.21(2)	0.24(1)	2.53(1)
Extrap.	0.47(1)	4.10(2)	0.25(1)	2.45(1)

**Table 5.** Best estimates of the exponent  $\nu$ , based on the behaviour of  $\langle r^2 \rangle(N)$ , and the asymptotic exponents  $t$  and  $\theta$  for a RdC model, based on our estimates from the ratios of the reduced moments.

Dimension	$\nu$	$t$	$\theta$
2D	0.750(2)	4.05(5)	0.49(1)
3D	0.592(2)	2.39(3)	0.29(4)

systems and second to qualitatively examine the size-dependence of the exponents.

We used an iterative routine which minimized the fitted  $\chi^2$  for each chain length. The first point to note is that the quality of the fits as judged by the  $\chi^2$  value is actually rather poor. Not surprisingly, the ansatz does not ideally describe the data—stated otherwise, this means that our data are precise enough to show this. The question remains whether it provides a useful approximation. Judged from figures 2 and 3 the answer is certainly positive. The fit results for  $N = 160$  are shown as broken lines in figures 2 and 3. We see that the fitted RdC distributions well describe the entire distribution. This is reassuring as the RdC ansatz was suggested by investigations of the limiting behaviour for small and large separations of the end points only. To be more quantitative, we used (11) to calculate reduced moments from the fitted RdC distributions and compared these values to the directly measured moments. All results for  $N > 100$  agreed within the error bars with the direct measurements (tables 2 and 3), while for  $N < 100$  the results were still very close. We note that for short chains the effect of working on a lattice is much stronger for the end-to-end distance distribution itself than for averaged quantities such as the moments.

We have summarized the best-fit parameters  $t_N$  and  $\theta_N$  in table 5. They are ‘in the right ballpark’ and show the expected chain-length dependence. The values we find for  $t$  decrease only slowly towards the expected exponents. In particular, it suggests that for a description of medium sized chains (and presumably also of many experimental systems) using a RdC model,  $t$  may not be equal to the theoretically expected values in table 1.

Finally we wish to know the behaviour for larger  $N$ . Extrapolating these data is difficult, in part because the relative errors are large and because, for small systems, the data are not well modelled by the RdC ansatz. More importantly, there is no *a priori* reason why the parameters of this approximate model should show any simple  $N$  dependence. This is

unlike the case for the reduced moments, where a power-law dependence is expected from scaling arguments. Therefore as a very crude estimate we used a simple  $1/N$  extrapolation, and have included the results at the bottom of table 4. Although these are close to the theoretical values in table 1 we emphasize that this procedure is not rigorous. In particular, the quoted margins of error account only for the statistical error. In the next section we present a more reliable method, based on the reduced moments.

### 3.3. Estimating model distributions from reduced moments

Because of the problems mentioned above we developed a method to estimate the best-fit parameters of a model distribution from the known reduced moments of the data. The advantage is that we believe we can reliably extrapolate the reduced moments, so that such a procedure allows us to reliably extend our investigation beyond the range of chain lengths studied by simulation.

To illustrate this approach consider the following example: in an experiment random numbers are drawn from a RdC distribution characterized by exponents  $\theta_{\text{true}}$  and  $t_{\text{true}}$ . We now attempt to describe these data using another RdC model for which  $t$  is set to a fixed value  $t_{\text{model}}$ . The optimal value of the parameter  $\theta_{\text{model}}$  is determined by fitting to the data via a  $\chi^2$  minimization:

$$\chi^2 = \int dx x^2 \frac{(q_{\text{true}}(x) - q_{\text{model}}(x))^2}{q_{\text{true}}(x)}. \quad (16)$$

Now suppose that we do not have the full distribution, but only its moments  $\delta_{pq}^{\text{true}}$ . Estimates,  $\theta_{\text{est}}^{pq}$ , of the best-fit parameter can be obtained from the condition that a particular reduced moment of the data is reproduced correctly by the model, i.e.

$$\delta_{pq}^{\text{true}} = \delta_{pq}(\theta_{\text{est}}^{pq}, t_{\text{model}}) \quad (17)$$

where the  $\delta_{pq}$  on the right-hand side is calculated from (11). (Note that, in this particular example, the left-hand side is similarly calculated since  $\delta_{pq}^{\text{true}} = \delta_{pq}(\theta_{\text{true}}, t_{\text{true}})$ ). It is a simple numerical task to invert (17) to determine  $\theta_{\text{est}}^{pq}$ .

In an experiment  $\delta_{pq}^{\text{true}}$  will only be known up to some  $\sigma_{pq}$ . The *statistical* error of  $\theta_{\text{est}}^{pq}$  can be obtained by repeating the inversion procedure for a value  $\delta_{pq}^{\text{true}} \pm \sigma_{pq}$ . The key point, however, are the *systematic* errors in the estimates obtained from the reduced moments, as we shall see below.

The use of this approach is demonstrated in figure 4. Here we fixed  $\theta_{\text{true}} = 0.25$  and  $t_{\text{model}} = 2.445$  and show how the best estimate for  $\theta_{\text{est}}^{pq}$  depends on both the *true* exponent  $t_{\text{true}}$  (varied from 2.3–2.6) and the particular moment  $\delta_{pq}^{\text{true}}$  we choose to invert. For  $\sigma_{pq}$  we took typical values from table 3, i.e. we assumed a precision in the moments similar to that of our simulations. The bands show the range in estimates for  $\theta_{\text{est}}^{pq}$  based on these assumed errors. Finally the full curve gives the ideal estimate for  $\theta_{\text{model}}$  obtained by using (16) to fit to the complete end-to-end distribution.

A comparison of the estimates  $\theta_{\text{est}}^{pq}$  to the optimal  $\theta_{\text{model}}$  shows that the method is quite successful, and that the results from different moments provide a useful consistency check for the applicability of the chosen model. The following four properties are apparent: (i) The lowest reduced moment,  $\delta_{21}$ , provides the best estimate, and for precisions typical of our simulations and extrapolations the optimal value is inside the error bars of the prediction for the range  $|t_{\text{true}} - t_{\text{model}}| < 0.05$ . (ii) The better the model ( $t_{\text{true}} \rightarrow t_{\text{model}}$ ) the better the estimates. (iii) For uncorrelated  $\delta_{pq}$  the variation of  $\theta_{\text{est}}^{pq}$  with the order of the moment is a

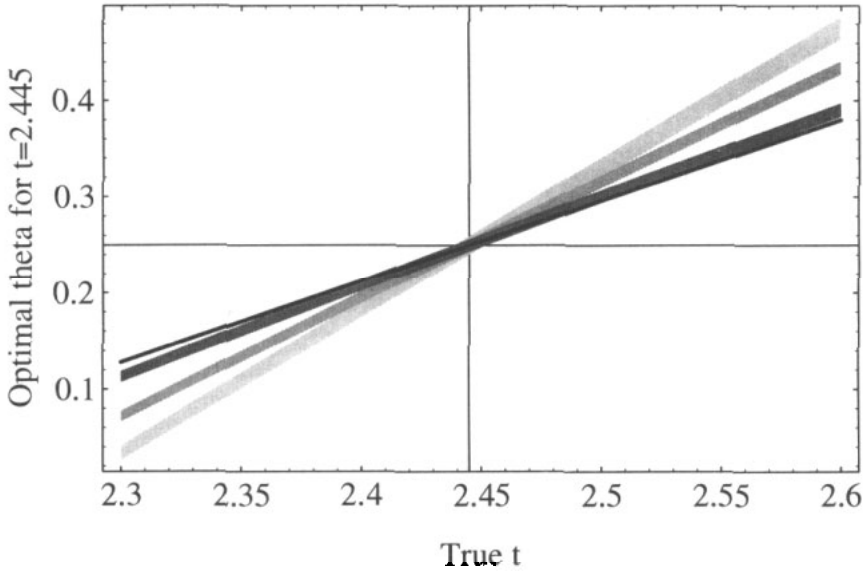


**Figure 4.** Test example for the estimation of a fit to a model function. The raw data were generated following a RdC distribution with  $\theta_{\text{true}} = 0.25$  and variable  $t_{\text{true}}$  (the  $x$ -axis of the figure). These data were then modelled using a RdC distribution with  $t_{\text{model}} = 2.445$  and  $\theta_{\text{model}}$  as an adjustable parameter. The black line shows the optimal  $\theta_{\text{model}}$  as obtained from a fit to the full end-to-end distribution. The shaded areas show, from dark to light gray, estimates of  $\theta_{\text{model}}$  based on inverting the three different reduced moments  $\delta_{21}$ ,  $\delta_{42}$ , and  $\delta_{82}$ . The width of the bands denotes the margins of error.

measure of the quality of the model: if there is little variation the model is better. (iv) The statistical error of  $\theta_{\text{est}}^{pq}$  grows with the order of the reduced moment.

In the following we apply this method to the reduced moments of our measured end-to-end distance distribution. Instead of the data listed in tables 2 and 3, however, we use the moments predicted by our numerical extrapolations. This offers two advantages: results can be obtained for arbitrary  $N$  to the precision of our extrapolation, and systematic correlations between the different reduced moments for a given  $N$  should be smaller than in the original data. For the error estimates we varied the number of data points used in the extrapolations of the reduced moments. Thus we repeated the fits and omitted either the  $N = 10$  or the  $N = 200$  and 240 data points. This procedure reproduces the statistical errors given in tables 2 and 3 and is also sensitive to possible systematic errors in the extrapolations. Furthermore, it provides a simple way to obtain the correlations in the estimates of  $\theta$  and  $t$ . We will consider two RdC models: first the one we used in our own fits with  $\theta$  and  $t$  as adjustable parameters and secondly a model similar to that of Eizenberg and Klafter with  $t$  fixed to the theoretical value of 2.445.

With both  $\theta$  and  $t$  as adjustable parameters we have to simultaneously invert (11) for two different reduced moments. Figures 5 and 6 show the resulting estimates for  $t$  and  $\theta$  together with the results of our direct fits to the complete distributions (table 4). The two shaded areas represent the predictions based on the combinations  $\delta_{21}/\delta_{42}$  and  $\delta_{21}/\delta_{82}$ . They have a typical width of  $\pm 0.01$  for  $t$  and  $\pm 0.005$  for  $\theta$  and are in excellent agreement with the direct fits and each other. Note, that where the regions overlap all three moments are reproduced correctly within the statistical error, which, as we pointed out above, is an

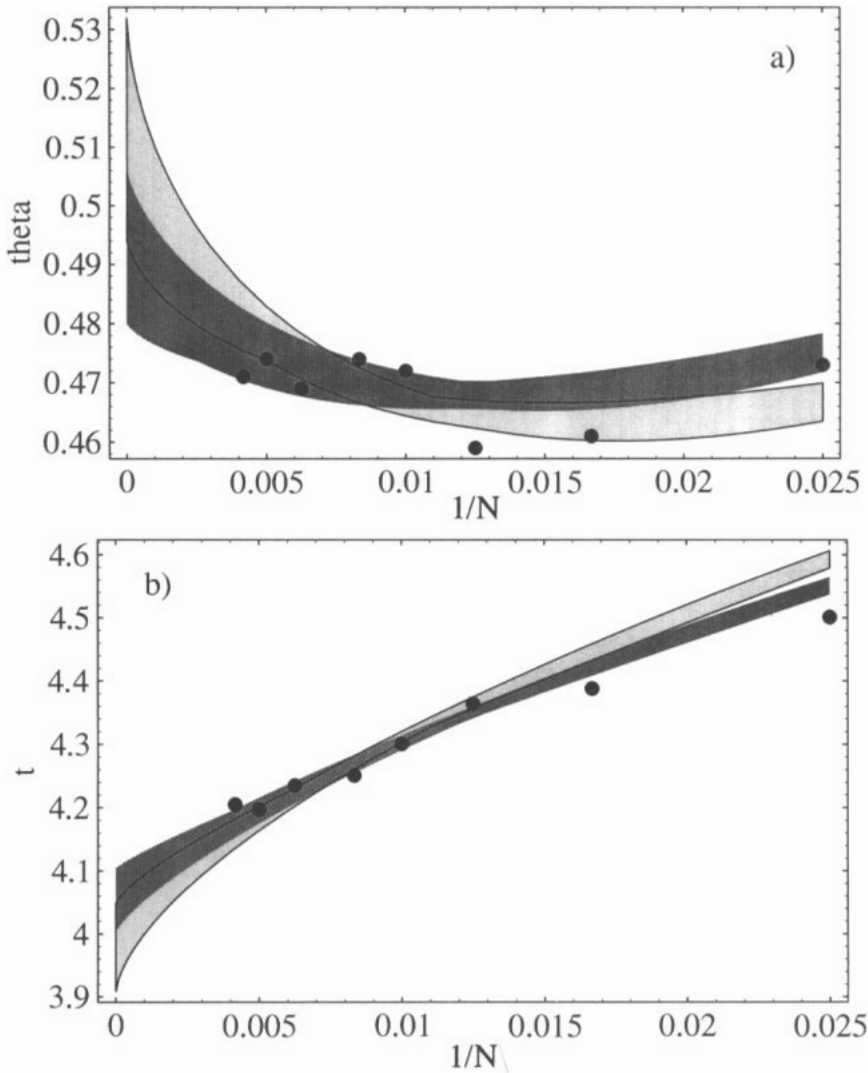


**Figure 5.** Effective exponents (a)  $\theta$  and (b)  $t$  as functions of chain length  $N$ , for  $d = 2$ , obtained by assuming the r<sub>0</sub>C distribution (7) and numerically inverting (11) simultaneously for two reduced moments. Shown are the combinations  $\delta_{21}(N)/\delta_{42}(N)$  (dark gray) and  $\delta_{21}(N)/\delta_{82}(N)$  (framed light gray). The  $\delta_{pq}(N)$  were calculated using our fit ansatz (15) with the exponents  $\Delta_{pq}$  listed in table 2. The full circles indicate the results from directly fitting the r<sub>0</sub>C function to the end-to-end distribution (from table 4).

indication of the appropriateness of the model. This gives a clue to the range of chain lengths over which the model is able to accurately represent the distributions. We also note that the plots of  $t$  and  $\theta$  as functions of  $1/N$  are clearly nonlinear, underlining the difficulty of directly extrapolating exponents obtained by fitting to the complete distribution.

It follows from figures 5 and 6 that we can expect the r<sub>0</sub>C model to work well for  $N > 50$  in 2D and for  $N > 100$  in 3D. Thus the analysis of the reduced moments confirms the impression conveyed from figures 2 and 3 and our findings from the direct fitting: that the overall behaviour of the end-to-end distance distributions can be modelled very well by

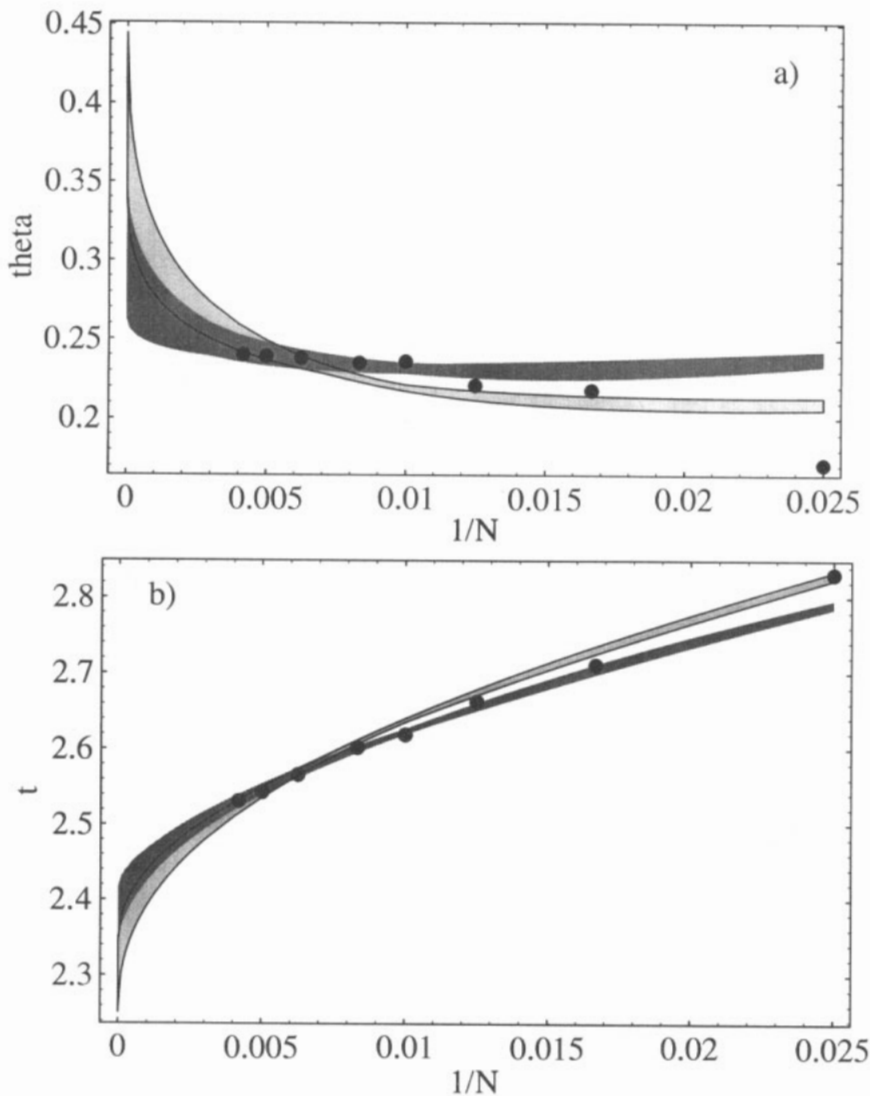


**Figure 6.** Effective exponents (a)  $\theta$  and (b)  $t$  as functions of chain length  $N$ , for  $d = 3$ , obtained by assuming the r&C distribution (7) and numerically inverting (11) simultaneously for two reduced moments. Shown are the combinations  $\delta_{21}(N)/\delta_{42}(N)$  (dark gray) and  $\delta_{21}(N)/\delta_{82}(N)$  (framed light gray). The  $\delta_{pq}(N)$  were calculated using our fit ansatz (15) with the exponents  $\Delta_{pq}$  listed in table 3. The dots indicate the results from directly fitting the r&C function to the end-to-end distribution (from table 4).

the r&C ansatz with  $t_N$  and  $\theta_N$  as chain length dependent parameters. Not surprisingly, the *exact* behaviour is more complicated. Indications were the poor  $\chi^2$  values of the direct fits mentioned earlier and differing estimates of the fit parameters based on combinations of higher moments such as  $\delta_{42}/\delta_{84}$ .

Our estimates of the optimal parameters for the asymptotic distribution listed in table 5 are based on the above analysis of the extrapolated moments. We subsequently used these

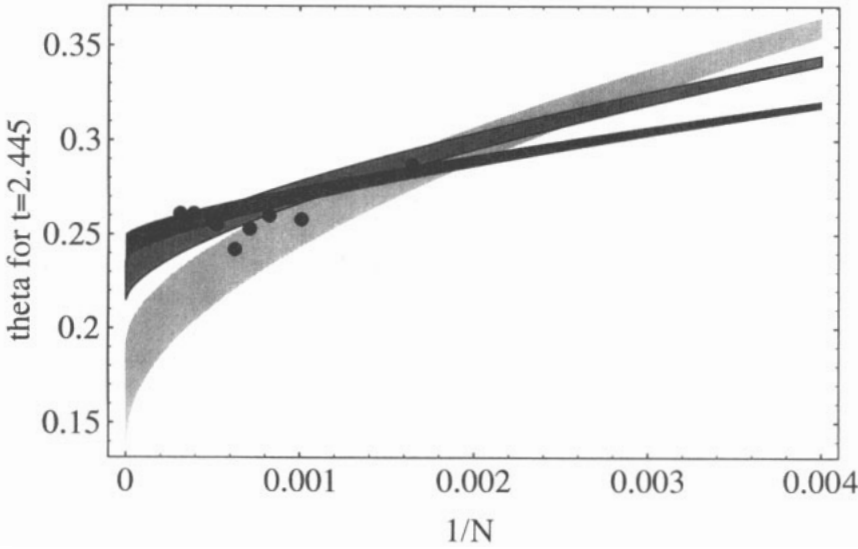


**Figure 7.** Effective exponents  $\theta^{\text{EK}}$  as a function of chain length  $N$  in 3D, estimated from our reduced moment data (and their extrapolations using (15) and the appropriate  $\Delta_{pq}$  from table 3). The  $\theta^{\text{EK}}$  were obtained by assuming an RdC distribution with  $t = 2.445$  and numerically inverting (11) for the four reduced moments  $\delta_{21}(N)$ ,  $\delta_{42}(N)$  and  $\delta_{82}(N)$  (from dark to light gray). The dots indicate the fit results of Eizenberg and Klafter [11, table V].

values to calculate reduced moments for an RdC description of the asymptotic distribution. The results are given in the rows labelled 'RdC(2)' in tables 2–4. They are in excellent agreement with the directly extrapolated values. The quoted errors are small as we took into account correlations between the estimates of  $t$  and  $\theta$ .

The estimated asymptotic exponents are in good agreement with the theoretically expected values, although, with comparatively large error margins. In two dimensions the high value of  $t_{2D}$  obtained by  $1/N$  extrapolation is corrected to a value  $t_{2D} = 4.05 \pm 0.05$ , while  $\theta_{2D} = 0.49 \pm 0.01$  is only a little bit higher than expected.

Things are more interesting in three dimensions. The value for  $\theta_{3D} = 0.29 \pm 0.04$  is in the expected range. However, we estimate  $t_{3D} = 2.39 \pm 0.03$ , with our results further indicating that the theoretically expected value of 2.445 is appropriate only for chain lengths around  $N = 600$ . The reader may recall the problems we had with the reduced moments of longer chains calculated from the Eizenberg and Klafter fits (figure 1). Only the first data points for  $N = 608, 800$  and  $992$  were in agreement with our extrapolations, while for longer chains the data did show a crossover to a constant value.

To demonstrate this point we now consider a RdC model with  $t$  fixed to the theoretical value 2.445, as was assumed by Eizenberg and Klafter [11]. The model has a single adjustable parameter,  $\theta^{\text{EK}}$ , which we estimate by inverting (11) for different  $\delta_{pq}$  of a given distribution†

Figure 7 shows the results of this procedure. The shaded areas show our predictions for  $\theta^{\text{EK}}(N)$  for  $N > 250$ , based on inverting four different reduced moments. The fit results of Eizenberg and Klafter [11, table V] are indicated by dots. They are quite scattered,

† EK actually needed to fit  $K$  as a second parameter, because they used  $N^\nu$  instead of the measured  $R_N$  as the scaling length. In this case (8) is no longer valid. However, (11) for the reduced moments still holds, allowing us to estimate  $\theta^{\text{EK}}$  independent of  $K$ . Note, that this means we are unable to account for their second fit parameter  $K$ .



but all within the range of our predictions. From our most reliable estimate based on  $\delta_{21}$  we expect a very weak chain length dependence of  $\theta^{\text{EK}}(N)$ . However, rather than saying that the distributions have reached their asymptotic shape we interpret this as an artefact of the model chosen to represent the data. The problems with the model are obvious from a comparison of the estimates based on different  $\delta_{pq}$ . As expected they all agree only near  $N = 600$ . The pattern is very similar to what we found in the test example (figure 4).

To understand the Eizenberg and Klafter data points in figure 1 we calculated a hypothetical curve  $\delta_{82}^{\text{EK}}(N)$  for RdC distributions with  $t = 2.445$  and our most reliable estimate for  $\theta^{\text{EK}}(N)$ . The results, shown as a dotted curve in figure 1, clearly mimic the behaviour of the EK data. Our line  $\delta_{82}^{\text{EK}}(N)$  crosses the straight line of our extrapolation around  $N = 600$ , ‘carrying along’ the data points of EK for longer chains.

As a last point we investigated whether or not the quality of our data were of sufficient quality to resolve the predicted change in the power-law exponent for free chains from  $\theta$  (equation (4)) for  $x \ll 1$  to  $g$  (equation (6)) for  $x \gg 1$ . In principle we could fit to selective regions of the data  $q(x)$  to extract the  $x$ -dependence of the exponents  $t$  and  $\theta$ . However, the success of this depends on our ability to extract these quantities from noisy data. The problem is not only the reduced database, but also that (8) and (9) are no longer valid so that  $K$  and  $C$  become additional fit parameters. To check whether or not such an approach is feasible we simulated a binning process for events following a Redner–des Cloizeaux distribution. The results were then subjected to the fitting process in order to recover the parameters  $t$  and  $\theta$  used to generate the test data. From this procedure we conclude that we cannot resolve the predicted change in the power-law exponent by fitting to our data, even if we were to significantly extend the precision of our results. Proper resolution of this question will require very high precision simulation studies of chains that are either stretched (by, for example, biased Monte Carlo sampling methods) or significantly longer than those studied here. This is even more true for the corrections to the limiting behaviour recently predicted by Stepanow [28] and mentioned in the introduction.

#### 4. Summary and discussion

In this paper we used Monte Carlo methods to investigate SAWs on square and cubic lattices in two and three dimensions, respectively. We obtained precise measurements of both the reduced moments of the end-to-end distance distributions and of the complete distributions themselves for several different chain lengths. We demonstrated that a simple  $1/N$  extrapolation of the reduced moments to infinite chain length does not describe our results. Instead we find that our data is best modelled by the functional form  $(a + bN^{-\Delta_{pq}})$  with moment-dependent correction to scaling exponents  $\Delta_{pq} < 1$  (figure 1). In particular, the approach to the asymptotic distribution is found to be slower than expected.

Our results confirm that the conjecture of Redner and des Cloizeaux (7) is a reasonable approximation for the measured end-to-end distance distribution. We find that an improved description is possible in the framework of a Redner–des Cloizeaux model by using chain-length-dependent effective exponents  $\theta_N$  and  $t_N$ . Such a model provides an excellent description of the end-to-end distance distributions (figures 2 and 3) provided the chains exceed a minimum length.

To obtain these distributions we binned our data into histograms and corrected for fluctuations in the number of accessible lattice points per bin. Careful analysis showed that the method becomes unreliable for bins very close to the origin. We believe that this explains observations of Dayantis and Palierne [10], who found deviations in their probabilities for  $r/N^v < 0.1$ .

We studied the predicted behaviour in the large- $N$  limit using our extrapolations for the reduced moments. These have the advantage of being both accurately measured and straightforward to extrapolate, unlike the effective exponents  $\theta_N$  and  $t_N$  themselves. We presented a method that allows us to extract estimates for the exponents, based on the reduced moments, and developed criteria for the reliability of this procedure. The resulting predicted behaviour in the large- $N$  limit yielded some surprising results: while, in general, the asymptotic values for the effective exponents were found to be close to the theoretical predictions of Fisher *et al* and des Cloizeaux, we obtained  $t = 2.39 \pm 0.03$  in three dimensions, which is quite different from the theoretical prediction  $t = 2.445$ . Note, that this is not in contradiction with the rigorous theoretical results, as they describe the behaviour of the asymptotic distributions in the limits of small and large  $x$ , whereas we aim to find the optimal parameters for an approximate model describing the entire distribution.

The result is nevertheless of practical importance as the value  $t = 2.445$  was assumed to be correct by Eizenberg and Klafter [11] in a study similar to ours, but involving significantly longer chains. The consequence is that their fits and the reduced moments calculated from them appear to show an unphysical 'plateau' at large  $N$ . The fact that extrapolations from our data predict a similar plateau for a model with  $t = 2.445$  is important evidence for the consistency of our methods.

We emphasize, that our ansatz for the reduced moments is empirical, leaving open the possibility of systematic errors in the extrapolation. The occurrence of moment-dependent correction to scaling exponents  $\Delta_{pq}$  certainly comes as a surprise, and cannot be explained as a simple finite-chain-length effect. It is an interesting question whether arguments along the line of Stepanow's work [28] could provide an explanation.

In any case, a direct calculation of reduced moments from the Eizenberg and Klafter data would provide an important check of our analysis. Also the subject should be addressable by exact enumeration and series extrapolation techniques. Independent of these issues we believe that the estimation and extrapolation of the optimal parameters for a model distribution from quantities such as the reduced moments should have applications beyond the current context.

## Acknowledgments

RE gratefully acknowledges helpful discussions with K Kremer, the hospitality of McGill University, and financial support by the Studienstiftung des deutschen Volkes.

## References

- [1] Redner S 1980 *J. Phys. A: Math. Gen.* **13** 3525
- [2] des Cloizeaux J and Jannink G 1987 *Les Polymères en Solution Les Editions de Physique* (Les Ulis)
- [3] de Gennes P G 1979 *Scaling Concepts in Polymer Physics* (Ithaca, NJ: Cornell University Press)
- [4] Kremer K and Binder K 1988 *Comput. Phys. Rep.* **7** 259
- [5] Pincus P 1976 *Macromolecules* **9** 386
- [6] Fisher M E 1966 *J. Chem. Phys.* **44** 616
- [7] McKenzie D S and Moore M A 1971 *J. Phys. A: Math. Gen.* **4** L82
- [8] des Cloizeaux J 1974 *Phys. Rev. A* **10** 1665
- [9] Bishop M and Clarke J H R 1991 *J. Chem. Phys.* **94** 3936
- [10] Dayantis J and Paliere J-F 1991 *J. Chem. Phys.* **95** 6088
- [11] Eizenberg N and Klafter J 1993 *J. Chem. Phys.* **99** 6088
- [12] Suzuki K 1968 *Bull. Chem. Soc. Japan* **41** 538
- [13] Alexandrowicz Z 1969 *J. Chem. Phys.* **51** 561
- [14] Alexandrowicz Z and Accad Y 1971 *J. Chem. Phys.* **54** 5338

- [15] Lal M 1967 *Mol. Phys.* **17** 57
- [16] Madras N and Sokal A D 1988 *J. Stat. Phys.* **50**
- [17] Domb C 1963 *J. Chem. Phys.* **38** 2957
- [18] Grassberger P 1982 *Z. Phys.* B **48** 255
- [19] MacDonald B, Jan N, Hunter D L and Steinitz M O 1982 *J. Phys. A: Math. Gen.* **18** 2627
- [20] Djordjevic Z V, Majid I, Stanley H E and dos Santos R J 1983 *J. Phys. A: Math. Gen.* **16** L519
- [21] Lyklema J W and Kremer K 1985 *Phys. Rev. B* **31** 3182
- [22] Nienhuis B 1982 *Phys. Rev. Lett.* **49** 1062
- [23] Le Guillou J C and Zinn-Justin J 1977 *Phys. Rev. Lett.* **39** 95
- [24] Wilson K G 1972 *Phys. Rev. Lett.* **28** 548
- [25] Guttmann A J 1987 *J. Phys. A: Math. Gen.* **20** 1839
- [26] Wall F T, Windwer S and Gans P J 1963 *J. Chem. Phys.* **38** 2220
- [27] Everaers R 1991 *Diploma thesis* TU Munich
- [28] Stepanow S 1990 *J. Physique* **51** 899